SCIENCE CHINA
Technological Sciences

• Article •

January 2015 Vol.58 No.1: 158–162
doi: 10.1007/s11431-014-5735-6

Slicing-response model for ablation mass removal of polyformaldehyde irradiated by pulsed CO_2 laser in vacuum

LI Gan, CHENG MouSen & LI XiaoKang*

National University of Defense Technology, College of Aerospace Science and Engineering, Changsha 410073, China

Received January 8, 2014; accepted October 9, 2014; published online December 18, 2014

The interaction between CO_2 laser and polyformaldehyde (POM) is quite important in the research of laser irradiation effects and mechanisms. At this time, the accuracy of the existing mass-ablation models for POM irradiated by CO_2 laser is poor compared with the experimental data. Based on the energy distribution deposited in the POM target, the active area excited by laser is divided into four slices, the ablation slice (the temperature-rising slice, the perturbation slice, and the undisturbed slice), and a slicing response model for the mass ablation of POM induced by pulsed CO_2 laser irradiation in vacuum is developed. A formula is deduced to predict the ablated mass areal density from the model and is verified with data from several studies and our own experiments. The results show that our model fits the experimental data quite well before the shielding effect of ablation products becomes notable. The applicability of the model to other materials and the mass ablation in atmosphere are also briefly explored.

laser ablation, pulsed CO_2 laser, polyformaldehyde (POM), ablation model

Citation: Li G, Cheng M S, Li X K. Slicing-response model for ablation mass removal of polyformal-dehyde irradiated by pulsed CO_2 laser in vacuum. Sci China Tech Sci, 2015, 58: 158–162, doi: 10.1007/s11431-014-5735-6

1 Introduction

Since the 1980s, polyformaldehyde (POM) has been widely studied as a laser propulsion propellant paired with CO_2 laser radiation [1,2]. Much recent work in the fields of laser machining [3] have also covered the subject of POM ablation by CO_2 laser. However, the ablation mechanism of POM irradiated by pulsed CO_2 laser is extremely complex [4], and efforts are still being made to find a model for propulsion performance prediction that is both simple and more applicable.

Sinko, Gregory, Phipps et al. [5,6] have presented two phenomenological models for laser-ablation mass removal of POM. These photochemical (1) and photothermal (2) models can be expressed as

$$\text{Photochemical}: \quad \mu = \frac{\rho}{\alpha}\ln\left(\frac{\Phi}{\Phi_{\text{th}}}\right), \tag{1}$$

$$\text{Photothermal}: \quad \mu = 2\rho\sqrt{D\tau\ln\left[\frac{(1-R)\Phi}{2\rho C_{\text{p}}\sqrt{\pi D\tau}T_{\text{b}}}\right]}, \tag{2}$$

where ρ is density; C_{p} is the heat capacity at constant pressure; α is the absorption coefficient; Φ is the laser fluence; Φ_{th} is the threshold fluence for ablation; τ is the laser-pulse time length; D is the thermal diffusion coefficient; and T_{b} is the boiling point. However, the results of eqs. (1) and (2) are quite different from the experimental data provided by Schall [7], Watanabe [8] and Sinko [9]. It is speculated that the ablation-surface movement may have a significant effect on the ablation process [10,11], especially when the laser fluence is extremely intense. This is the point that is ignored

*Corresponding author (email: lxk0330@gmail.com)

in both the above mentioned models. Moreover, the photochemical model requires the photon energy and the chemical bond energy to be equivalent and for the photon energy of CO_2 laser is only about 1/32 of the bond energy of POM(-C-O-). Therefore, the photothermal mechanism is a more reasonable ablation mechanism for the description of the ablation of POM.

In this paper, our efforts are mainly focused on the correction of the physical model for the ablation mass removal of POM irradiated by CO_2 laser. A slicing response model with modified threshold fluence as slicing ablation criterion is proposed to describe the laser-induced mass removal process. We also performed experiments on the ablation of POM irradiated by high-fluence CO_2 laser to verify the validity of the corrected model. To avoid the complex cases of ablation in an ambient atmosphere, the model and experiments were all carried out in vacuum, which is also our application aim.

2 Mass removal model of POM ablation

A schematic of the laser-induced ablation process of POM is shown in Figure 1. We begin our discussion of the ablation model with the propagation of a laser beam in solid POM, which is governed by the Bouguer-Lambert-Beer absorption law:

$$I = I_0 \exp(-\alpha x), \tag{3}$$

where α is the absorption coefficient; I_0 is the incident laser intensity; and x is the distance to the ablation surface. As the laser energy deposited in the POM increases, the temperature rises rapidly and a layer is ready to ablate (Figure 1(b)). When the fluence is greater than the ablation threshold, the ablation is initiated and the resultant ablation product is emitted outward (Figure 1(c)). During emission, the ablation product interacts with the incident laser beam (Figure 1(d)). When the laser intensity is large enough, the product becomes ionized and damps the incoming laser beam that finally arrives at the ablation surface.

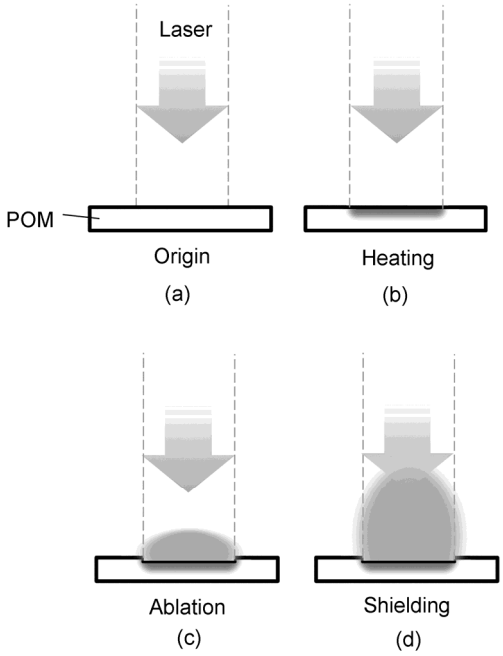

Figure 1 Schematic diagram of laser-induced ablation of POM.

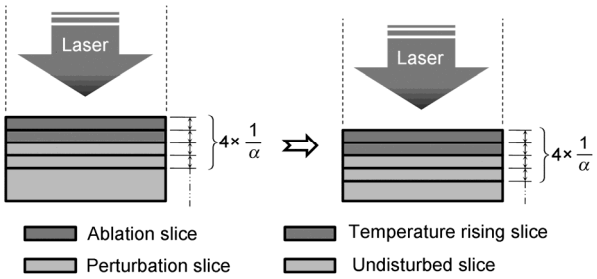

Figure 2 Schematic diagram of the slicing-response model.

2.1 Slicing-response model

Based on the above analysis, we envisioned a slicing- response model for the ablation of POM. It consists of four slices: the ablation slice, the temperature-rising slice, the perturbation slice, and the undisturbed slice (Figure 2). The ablation slice denotes the region that is going to ablate; the temperature-rising slice is the one beneath the ablation slice, in which the temperature is obviously higher than the ambient temperature; the perturbation slice is defined as the area in which the state parameters are slightly changed by the thermo-mechanic disturbance; and the undisturbed slice is the layer that retains the initial state. In order to illustrate the function of each slice, the thickness is defined as $1/\alpha$, which is also convenient for mathematical treatment. Based on the definition and according to eq. (3), $(1-1/e) = 63.2\%$ of the incident laser energy is deposited in the ablation slice; $(1/e-1/e^2)=23.3\%$ is deposited in the temperature rising slice; $(1/e^2-1/e^3)=8.6\%$ is deposited in the perturbation slice, and $(1/e^3-1/e^4)=3.1\%$ is deposited in the undisturbed slice. It is obvious that the distribution proportion of the laser energy deposited in the different slices is consistent with the definition of each slice. The ablation process can be expressed as follows.

2.1.1 Initial Ablation

When the cumulative laser energy per unit area of the irradiated POM surface reaches the ablation criterion for the whole slice Φ_{cr} (the Φ_{cr} will be discussed in detail in Section 2.2), the ablation slice breaks off instantaneously. Counting from the beginning of irradiation, the initial ablation will need a time of

$$\tau_1 = \Phi_{cr} / I_0 . \tag{4}$$

Meanwhile, the temperature-rising slice continues to be heated.

2.1.2 Continued ablation

After the ablation slice has been ablated, the resultant temperature-rising slice becomes the new ablation slice. Because the new slice has already absorbed some energy, about Φ_{cr}/e, e is the Euler's number and the irradiation time needed for ablation is

$$\tau_2 = \left(\Phi_{cr} - \frac{\Phi_{cr}}{e}\right)\Big/ I_0 = \left(1-\frac{1}{e}\right)\tau_0, \tag{5}$$

where, $\tau_0 = \tau_1$ is defined as the reference time for ablation.

Similarly, the irradiation time needed for ablation of the third ablation slice is

$$\tau_3 = \left(1-\frac{1}{e}+\frac{1}{e^2}\right)\tau_0. \tag{6}$$

The irradiation time needed for ablation of the n^{th} ablation slice is

$$\tau_n = \left[1-\frac{1}{e}+\frac{1}{e^2}+\cdots+\frac{(-1)^{n-1}}{e^{n-1}}\right]\tau_0. \tag{7}$$

The total irradiation time Θ_n for ablation of all the n slices is

$$\begin{aligned}\Theta_n &= \sum_{i=1}^{n}\tau_i = \left[n-(n-1)\frac{1}{e}+(n-2)\frac{1}{e^2}+\cdots+\frac{(-1)^{n-1}}{e^{n-1}}\right]\tau_0 \\ &= \left[\frac{en}{e+1}+\frac{e+\dfrac{(-1)^{n-1}}{e^{n-1}}}{(e+1)^2}\right]\tau_0.\end{aligned} \tag{8}$$

Then, we may calculate the ablated mass areal density as follows

$$\mu_m = \frac{\rho}{\alpha}\left\{n+\left[\left(\tau-\Theta_n\right)/\tau_{n+1}\right]\right\},\ \Theta_n < \tau < \Theta_{n+1}. \tag{9}$$

The average velocity of the surface ablation progression is

$$U_a = n/\alpha\Theta_n. \tag{10}$$

When $n \gg 1$;

$$\begin{cases}\Theta_n = \sum_{i=1}^{n}\tau_i \approx n\dfrac{e}{1+e}\tau_0, \\ U_a = (1+e)/\alpha e\tau_0, \\ \mu_m = \dfrac{e+1}{e}\dfrac{\rho}{\alpha}\dfrac{\tau}{\tau_0}.\end{cases} \tag{11}$$

2.2 Slicing-ablation criterion

Because we have used the slicing-response assumption in this model, a slicing-ablation criterion is needed to make the model self-consistent. We denote this value as Φ_{cr} to represent the laser fluence needed for the ablation of a slice with a depth of $1/\alpha$. Firstly, let us focus on the energy balance of the infinitesimal layer beneath the ablation surface (Figure 3(a)).

The energy deposited in the layer is utilized for temperature rising, fusion, and decomposition. When the laser fluence reaches the ablation threshold Φ_{th}, the energy conservation relationship is of the form

$$\begin{aligned}&(1-R)\left[\Phi_{\text{th}} - \Phi_{\text{th}}\exp(-\alpha\Delta x)\right] \\ &= \rho\Delta x\left(C_p\cdot\Delta T_g + L_m + L_d\right),\end{aligned} \tag{12}$$

where ΔT_g is the difference between the initial and the vaporization temperature of POM; L_m is the latent heat of fusion; L_d is the heat of decomposition; and R is the reflectivity. In eq. (12) we have neglected the effect of thermal conduction, because the thermal conductivity of POM is just about 0.25 W/(m·K)[9]. Thus we can get

$$\Phi_{\text{th}} = \frac{\rho}{\alpha(1-R)}\left(C_p\cdot\Delta T_g + L_m + L_d\right), \quad \Delta x \to 0. \tag{13}$$

We assume that the ablation depth h is directly proportional to the laser-fluence difference (Φ–Φ_{th}). Thus, as shown in Figure 3(b), we have

$$\Phi_{\text{th}} + \Phi_2 = 2\Phi_{\text{cr}}, \tag{14}$$

where Φ_2 is the laser fluence that corresponds to the ablation depth of $2/\alpha$ and can be expressed as

$$\Phi_2 = \left(\tau_1+\tau_2\right)I_0 = \left(2-\frac{1}{e}\right)\Phi_{\text{cr}}. \tag{15}$$

Therefore, Φ_{cr} is of the form:

$$\Phi_{\text{cr}} = e\Phi_{\text{th}} = \frac{\rho e}{\alpha(1-R)}\left(C_p\cdot\Delta T_g + L_m + L_d\right). \tag{16}$$

3 Experimental

The schematic diagram of experimental setup is shown in Figure 4. The experiments were carried out in a vacuum

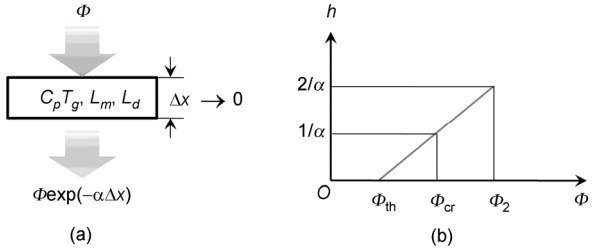

Figure 3 Schematic diagram for theanalysis of Φ_{cr}.

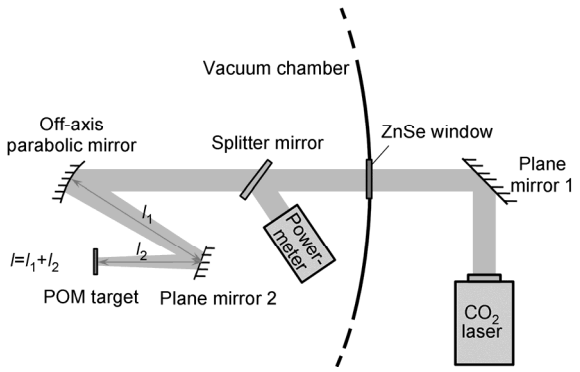

Figure 4 Schematic diagram of experimental setup.

chamber with a background pressure of about 10^{-1} mbar. A transversely excited atmospheric CO_2 laser (HUST, Wuhan) was used for this investigation. The wavelength and pulse time width were 10.6 μm and 5 μs, respectively. The laser beam was guided into the chamber through a ZnSe window and small parts were coupled out by a splitter mirror for integral pulse-energy monitoring. The majority of the transmitted beam was focused using an off-axis parabolic mirror and different intensities were obtained by adjusting the distance between POM target and the off-axis parabolic mirror. The laser pulse energy is monitored with a Scientech Astral 380802 calorimetric power/energy meter (Germany) wuth a fixed calibration factor. The ablation mass removal was measured using an electronic balance with a precision of 0.01 mg. The investigated fluence varied between 30 and 200 J/cm^2.

The target is a 2 mm thick white POM foil (Dupont, Germany). The material parameters are given in Table 1.

4 Results and discussion

Our experimental and calculated data of ablated mass areal density are shown in Figure 5, which includes plots of the experimental results from AVCO Everett research lab (AVCO) [14], Nagoya University (NU) [6,15] and Tohoku University (TU) [8]. It can be seen that the calculated data agree well with the experimental data for the fluences from about 0.7 J/cm^2 until about 35 J/cm^2, after which the deviations become obvious. It is believed that the ablation products began to damp the incident beam seriously when the fluence was larger than 35 J/cm^2 [9], because the ablation products were obviously ionized into plasma, and the plasma is a good absorber of the incident laser. According to eq. (13), the calculated ablation threshold (0.70 J/cm^2) is slightly larger than the experimental value (0.51 J/cm^2) [6]; therefore, the calculated results are slightly smaller. In Figure 5, the dashed line and dash-dotted line denote the predictions of photochemical (eq. (1)) and photothermal (eq. (2)) models, respectively. Compared with these two models, the slicing-response ablation model we have developed can give more-satisfying predictions.

Table 1 Main material parameters of POM [12,13]

ρ (kg/m^3)	C_p (J/kgK)	α (m^{-1})	T_b (K)	L_m (J/kg)	L_d (J/kg)
1420	1500	6.74×10^5	642	2.0×10^5	2.17×10^6

Although the slicing-response ablation model was developed for POM, it is expected to apply to other materials as well. Figure 6 shows the plots of the ablated mass areal density versus laser fluences for C, PI, and PS [17–19]. The data for C was obtained in vacuum; the data for PI and PS were obtained in the atmosphere of 1 atm. Because new energy sources such as oxidation and combustion appear in atmosphere, we used the actual measured value of Φ_{th} in our calculations for PI and PS. The Φ_{th} of PI and PS are 0.09 J/cm^2 [18] and 3.8 J/cm^2 [19] respectively. Other parameters are listed in Table 2. Our model can properly describe the variation tendency of μ. As for C, due to its extremely high boiling point, the conspicuous shielding effect turns up when Φ>8 J/cm^2. It is noticeable that the outcome of eq. (13) is much larger than the experimental value [20], which will limit the applicability when the fluence is close to the Φ_{th}. It is noteworthy that the slicing response ablation model fits the PI data better than the PS data; this result is attributed to the vast difference between the absorption coefficient of PI for 308 nm laser and that of PS for 6.25 μm laser.

5 Conclusions

Based on the energy deposition distribution of CO_2 laser propagation of POM, we developed a slicing response-

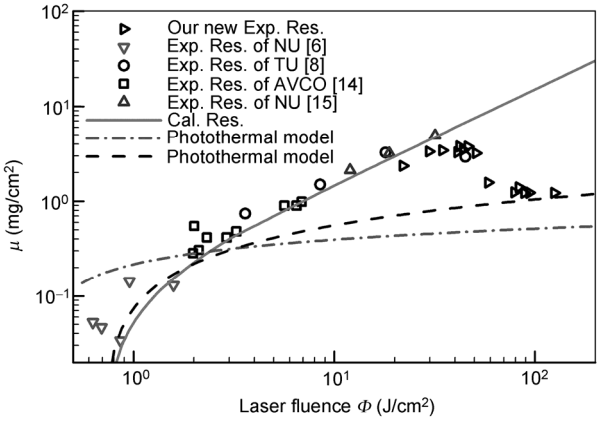

Figure 5 Ablated mass areal densities for different fluences.

Table 2 Material parameters of C, PI and PS [13,16]

Material	ρ (kg/m^3)	C_p (J/kgK)	α (m^{-1})	T_b (K)	L_m (J/kg)	L_d (J/kg)	λ (μm)
C [17]	2250	710	1.5×10^7	4473	–	5.97×10^7	1.06
PI [18]	1420	1100	1.0×10^7	711	5.5×10^4	1.39×10^6	0.308
PS [19]	1050	1300	1.97×10^4	700	–	1.0×10^6	6.25

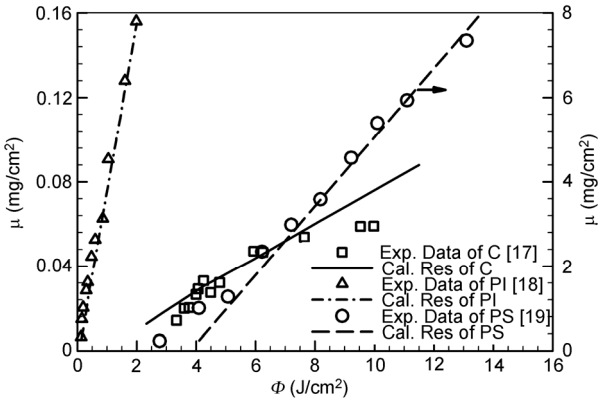

Figure 6 Application of slicing response ablation model to other materials.

model to simulate the CO_2 laser-induced mass removal process of POM. A formula was deduced for the prediction of the ablated mass areal density from the model and was verified against data from several studies and our own experiments in high-fluence regions. The main conclusions can be summarized as follows: 1) The slicing response model can give more-satisfying predictions of the ablation mass removal of polyformaldehyde (POM) irradiated by pulsed CO_2 laser in vacuum, until the shielding effect of ablation products becomes notable at about Φ>35 J/cm^2; and 2) The slicing response model has good applicability to other materials, particularly when the absorption coefficient of the target is adequately large. The model can also be used for laser-induced ablation in atmosphere, but an actual measured ablation threshold is needed as an input parameter.

This work was supported by the National Natural Science Foundation of China (Grant No. 51306203) and the Advancing Research Program of NUDT (Grant No. JC14-01-02).

1 Ageichik A A, Repina E V, Rezunkov Y A, et al. Detonation of CHO working substances in a laser jet engine. Tech Phys, 2009, 54: 402
2 Phipps C, Birkan M, Bohn W, et al. Review: laser ablation propulsion. J Propul Power, 2010, 26: 609–637
3 Pfleging W, Baldus O, Bruns M, et al. Photon Processing in Microelectronics and Photonics IV. WA: Bellingham, 2005. 479
4 Lippert T. Laser application of polymers. Adv Polym Sci, 2004, 168: 51–246
5 Sinko J E, Gregory D A. Models for laser ablation mass removal and impulse generation in vacuum. AIP Conf Proc, 2010, CP1230: 193–203
6 SinkoJ E, Phipps C R, Tsukiyama Y, et al. critical fluences and modeling of co_2 laser ablation of polyoxymethylene from vaporization to the plasma regime. AIP Conf Proc, 2010, CP1230: 395–407
7 Schall W O, Eckel H A, Tegel J, et al. Properties of laser ablation products of delrin with co_2 laser. Final Report (EOARD Grant, Cooperative Award) No. FA8655-03-1-3061, 2004
8 Watanabe K, Mori K, Sasoh A. Ambient pressure dependence of laser-induced impulse onto polyacetal. J Propul Power, 2006, 22(5): 1150–1153
9 Sinko J E, Sasoh A. Review of co_2 laser ablation propulsion with polyoxymethylene. Int J Aerospace Innovat, 2011, 3: 93–130
10 Bäuerle D. Laser Processing and Chemistry. 3rd ed. Berlin: Springer Verlag, 2000
11 Bityurin N, Luk'yanchuk B S, Hong M H, et al. Models for laser ablation of polymers. Chem Rev, 2003, 103: 519–552
12 SinkoJ E. Vaporization and Shock Wave Dynamics for Impulse Generation in Laser Propulsion. Dissertation of Doctoral Degree. Huntsville: The University of Alabama in Huntsville, 2008
13 Stoliarov S I, Walters R N. Determination of the heats of gasification of polymers using differential scanning calorimetry. Polym Degrad Stabil, 2008, 93: 422–427
14 Reilly D A. Laser Propulsion Experiments. Final Report, Everett: AVCO Research Lab, Inc. 1991
15 Suzuki K, Sawada K, Takaya R, et al. Ablative impulse characteristics of polyacetal with repetitive co_2 laser pulses. J Propul Power, 2008, 24(4): 834–841
16 Lyon R E, Quintiere J G. Criteria for piloted ignition of combustible solids. Combust Flame, 2007, 151: 551–559
17 Bulgakov A V, Bulgakova N M. Thermal model of pulsed laser ablation under the conditions of formation and heating of a radiation-absorbing plasma. Quantum Electronics, 1999, 29(5): 433–437
18 Sutcliffe E, Srinivasan R. Dynamics of uv laser ablation of organic polymer surfaces. J Appl Phys, 1986, 60(9): 3315–3322
19 Johnson S L, Bubb D M, Schriver K E. On the mechanism of resonant infrared polymer ablation: the case of polystyrene. Proc SPIE 7005, 2008, 70050G
20 Torrisi L, Borrielli A, Margarone D. Study on the ablation threshold induced by pulsed lasers at different wavelengths. Nucl Instrum Meth B, 2007, 255: 373–379